PAMM

SPECIAL ISSUE 95th Annual Meeting of the International Association of Applied Mathematics and Mechanics (GAMM)

RESEARCH ARTICLE OPEN ACCESS

Iterative Mold Adaptation for Pre-Compensation of Warpage in Aluminum Casting

Steffen Tillmann[1] | Shrujal Gor[2] | Stefanie Elgeti[1,3] | Andreas Bührig-Polaczek[2] | Björn Pustal[2]

[1]Chair for Computational Analysis of Technical Systems, RWTH Aachen University, Aachen, Germany | [2]Foundry Institute, RWTH Aachen University, Aachen, Germany | [3]Institute for Lightweight Design and Structural Biomechanics, TU Wien, Vienna, Austria

Correspondence: Steffen Tillmann (tillmann@cats.rwth-aachen.de)

Received: 23 June 2025 | **Accepted:** 4 December 2025

ABSTRACT

As a result of uneven cooling and internal stresses, warpage is a significant challenge in metal casting, particularly when using metal dies. Previous research has sought to reduce warpage by adjusting process parameters, such as the extraction temperature. An alternative approach involves modifying the mold cavity shape to compensate for expected deformation. While this compensation is often based on experience, numerical design optimization offers a systematic alternative. Various optimization methods have been developed for injection molding, but their application to metal casting remains less explored. In this study, we apply and compare two warpage compensation methods in metal casting: the reverse geometry method and a shape optimization-based approach. Both methods were initially developed for injection molding. We perform coupled thermomechanical simulations using the commercial software Abaqus. Each method is evaluated based on how it adapts the geometry, and we analyze their respective strengths and limitations across different scenarios. Using a simple test geometry, our results demonstrate that the reverse geometry method performs better regarding warpage reduction and computational costs, while the shape optimization-based method offers superior generalization.

1 | Introduction

Warpage remains a critical defect in casting processes, primarily arising from non-uniform cooling and the buildup of residual stresses [1]. While thermal management strategies—such as mold preheating, controlled casting temperatures, and conformal cooling channels—can enhance process robustness and reproducibility, recent studies indicate that they alone have limited impact on reducing final part distortions [2]. Instead, precise mold geometry and tailored design modifications have shown greater effectiveness in mitigating warpage, particularly in aluminum gravity die casting. For instance, specific geometric features like mold slopes, gating systems, riser dimensions, and core placements have been empirically validated to improve solidification behavior and dimensional accuracy [3]. These insights have led to developing pre-compensated molds, where geometry is intentionally modified based on predicted distortions [4]. However, achieving optimal mold geometry for complex parts requires sophisticated, iterative inverse design algorithms that can systematically converge on a mold configuration that minimizes warpage under real casting conditions.

In injection molding, similar approaches have been tried to reduce warpage. Here, warpage is also influenced by factors such as melt and mold temperatures and injection and holding pressures, as well as injection and cooling times, which can be optimized using various algorithms [5–9]. Additional measures, including localized cooling adjustments [10–12] and part design modifications (e.g., wall thickness) [13, 14], help mitigate warpage. Another effective strategy is to reshape the mold cavity to pre-compensate warpage [15].

Proposed methods for calculating the optimal cavity shape range from scaling approaches such as the 3D Volume Shrinkage Method [16] to inverse warpage models [17, 18], as well as iterative non-intrusive techniques including the reverse geometry method [19–21] and normal vector method [19]. Alternatively, shape optimization can be performed through free-form deformation [22] and Bayesian optimization [23, 24]. A comparative study [20] shows that the reverse geometry method converges rapidly, while the normal vector method performs slightly worse and adds unnecessary complexity to the algorithm. Full shape optimization is typically more resource-intensive but offers the ability to introduce additional goals on top of the geometric warpage compensation.

The reverse geometry method was adapted to work when the geometry is remeshed, and thus, the connectivity of the mesh changes. For this, an interpolation method is used to adjust the mesh nodes of the new mesh [21]. The difficulty with the aluminum casting simulation is that there are two meshes, one for the cast and one for the mold. While this is not a problem for the shape optimization method, the reverse geometry method must be adapted to handle both meshes. This will be explained in detail in Section 2.3.

To adapt the mold mesh to the updated cast geometry, a mesh morphing method is required [25, 26]. We employ a technique based on radial basis function (RBF) interpolation [27, 28], a method well-suited for multivariate interpolation tasks [29, 30]. RBF interpolation does not require the interpolation nodes to lie on a structured grid or have predefined connectivity, and it remains stable even with a large number of nodes in multiple dimensions. These properties make it particularly suitable for morphing large and complex meshes [27, 28]. The deformation can either be based on the whole surface mesh of the part, selected control points around the mesh, interior control points, or a combination. This has been applied for mesh morphing in shape optimization in ship hull [31], aerodynamics [32], and structural mechanics applications [33, 34].

The paper is structured as follows: First, the forward simulation model is explained. Then, the shape optimization and reverse geometry methods are presented, and how they are applied to the aluminum casting simulation. The results for both methods are shown and discussed, followed by a conclusion.

2 | Numerical Setup

2.1 | Forward FEM Simulation

In this study, a cast part with an L-shaped geometry is considered. The mold cavity is generated by performing a Boolean subtraction of the L-shaped geometry from a rectangular block using CAD operations. In subsequent iterations, the selected warpage compensation algorithm updates the mold and the cast. The warpage compensation algorithms used in this study are explained in Sections 2.2 and 2.3. This updated mold and the inverted cast geometry are then used as input for the next iteration.

We use the fully coupled thermal-stress analysis model of Abaqus [35] for the simulation. Here, we apply the principle of virtual work and the heat equation, which are fully coupled. The principle of virtual work to compute the displacement u is:

$$\int_V \boldsymbol{\sigma} : \delta\mathbf{D}\, dV = \int_S \mathbf{t}^T \cdot \delta\mathbf{v}\, dS + \int_V \mathbf{f}^T \cdot \delta\mathbf{v}\, dV, \tag{1}$$

where $\boldsymbol{\sigma}$ is the Cauchy stress tensor, $\delta\mathbf{D}$ is the virtual strain-rate tensor on the volume V. The traction stress $\mathbf{t}^T$ with the virtual velocity $\mathbf{v}$ is acting on the boundary S, and $\mathbf{f}^T$ is the body force. The heat equation to compute the temperature θ is:

$$\int_V \rho\dot{U}\, dV = \int_S q\, dS + \int_V r\, dV. \tag{2}$$

Here, ρ is the density, $\dot{U}$ is the time rate of change of internal energy, q is the heat flux per unit area, and r is the externally supplied heat per unit volume. Both equations are then fully coupled:

$$\begin{bmatrix} K_{uu} & K_{u\theta} \\ K_{\theta u} & K_{\theta\theta} \end{bmatrix} \begin{Bmatrix} \Delta u \\ \Delta\theta \end{Bmatrix} = \begin{Bmatrix} R_u \\ R_\theta \end{Bmatrix}, \tag{3}$$

where Δu and $\Delta\theta$ are the respective corrections to incremental displacement and temperature, K_{ii} are submatrices of the fully coupled Jacobian matrix, and R_u and R_θ are the mechanical and thermal residual vectors, respectively [35].

The initial temperature of the cast part is set at 720°C, while the mold is initialized at 300°C. Heat transfer between the cast and the mold occurs primarily through conduction, whereas heat is dissipated from the outer surfaces of the mold to the surrounding environment via natural convection. To simplify the mechanical boundary conditions and focus on the primary objective of evaluating inverse optimization techniques, both the cast and mold are constrained at the top surface. The computational mesh generated for this configuration, along with the geometrical and boundary conditions described above, is illustrated in Figure 1.

TABLE 1 | Chemical composition of aluminum alloy A356 (Mass-%).

Si	Fe	Cu	Mn	Mg	Zn	Ti	Other
6.5–7.5	0.12	0.02	0.05	0.3–0.45	0.07	0.18	Sr

The selected material for this investigation is the widely employed A356 aluminum alloy (see Table 1), prevalent in the casting industry. Temperature-dependent material properties, encompassing density, specific heat, elastic modulus, thermal conductivity, and expansion coefficient, essential for a comprehensive coupled simulation, were incorporated in the analysis. Information pertaining to the plastic behavior of the material was sourced from existing literature. It is noteworthy that plastic deformation is presumed to be independent of strain rate, given the exceedingly low strain rates observed in the gravity die casting process

2.2 | Shape Optimization Approach

In this first warpage compensation approach, the problem is formulated as a shape optimization task and addressed using

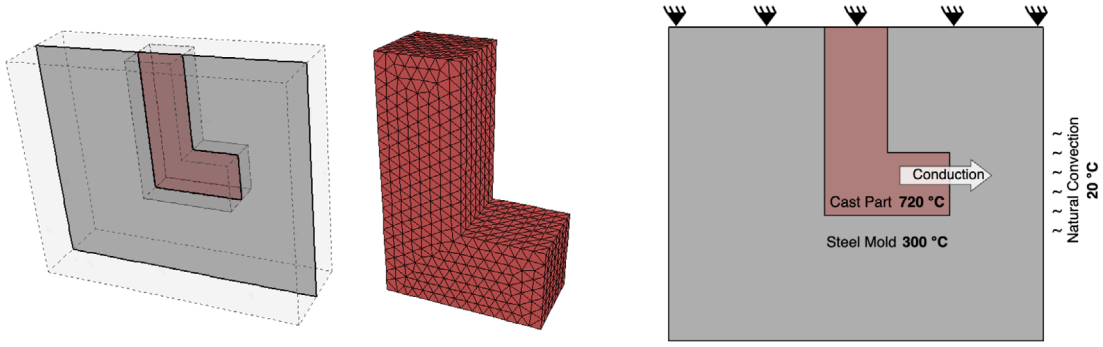

(a) Geometry and Mesh **(b)** Boundary Conditions

FIGURE 1 | The geometry, mesh, and boundary conditions of the cast and mold of the forward simulation model.

the COBYQA algorithm [36, 37]. COBYQA was chosen because it is derivative-free and remains computationally efficient when derivatives are unavailable, which is crucial since the Abaqus simulation model does not provide any derivatives of an objective function. How the shape optimization warpage compensation can be used in cavity design is described in detail in [24], with the notable difference that there, Bayesian optimization is used in place of COBYQA. Here, we give a brief recap. When approaching the warpage compensation problem as a shape optimization problem, the first ingredient that needs to be determined is the objective function J. Here, we use a function that computes the average of the squared distance between the ideal and deformed shapes at each mesh node on the part's surface. This yields:

$$J = \sqrt{\frac{1}{N}\sum_{j=0}^{N} ||\mathbf{x}_{\mathbf{ideal,j}} - \tilde{\mathbf{x}}_{\mathbf{j}}||_2^2}\,, \tag{4}$$

where $\mathbf{x}_{\mathbf{ideal}}$ and $\tilde{\mathbf{x}}$ are the mesh node coordinates of the ideal and deformed shapes. Additionally, N is the total number of mesh nodes, and j indicates the number of the mesh node. So, for each mesh node, the distance between the ideal shape and the warped shape is computed and averaged over the whole part by computing the root mean square error. This function thus measures the average squared difference between the ideal and the warped surface of the geometry and is also used to measure the algorithm's performance. For geometry deformation and parametrization, the free-form deformation method [22] is used, embedding the finite element mesh in a box-spline. We employ a quadratic B-spline with three evenly distributed control points in each coordinate direction. The COBYQA optimization begins with small deviations of each control point coordinate, and then each optimization step is based on a quadratic approximation. Additional objectives or constraints (e.g., avoiding hot cracks or other defects) can easily be included.

Only minor adjustments were necessary to adapt the method for aluminum casting. Both the cast and mold meshes are embedded into the same box spline, preserving their interface integrity. The adapted node coordinates for both meshes are then exported into the Abaqus input file for simulation.

2.3 | Reverse Geometry Method

Reference [20] demonstrated that the reverse geometry method delivered the best performance for warpage compensation in injection molding. However, adapting this method for casting simulation requires additional modifications to enable implementation and automation. Unlike injection molding, casting simulation involves both the cast and the mold, necessitating matching meshes for both components before the simulation can begin.

The original reverse geometry method provides an algorithm to adapt the mesh of the cast for the simulation. The vector $\mathbf{x}$ represents the mesh coordinates. Here, $\mathbf{x}_i$ denotes the mesh coordinates of the cavity shape in iteration i. The resulting warpage from the simulation model is denoted as $\tilde{\mathbf{x}}_i$ and the ideal shape as $\mathbf{x}_{ideal}$. The update scheme then reads:

$$x_0 = x_{ideal}\,, \tag{5}$$

$$x_{i+1} = x_{ideal} - (\tilde{\mathbf{x}}_i - \mathbf{x}_i)\,. \tag{6}$$

Adapting the mesh of the mold is more complicated. At the start of each iterative simulation run, a mesh of the mold that tightly fits around the cast is required so that the heat conduction from the cast to the mold works in the simulation model. When the shape of the cast is updated in the next iteration of the reverse geometry method, the mold does not automatically adjust to match it. As a result, the mesh nodes at the interface between the mold and the cast become misaligned. To address this, we must identify the interface mesh nodes of the mold and reposition them according to the updated cast mesh. Additionally, the internal mesh nodes of the mold need to be adapted using a mesh update method to maintain high mesh quality.

To compute the surfaces of the meshes and find the interface nodes between the cast and the mold, we use the Python library PyVista [38]. This library can compute the surface of a mesh and perform Boolean operations on meshes. This gives us the mesh nodes at the interface. With this, we can create a surface mesh consisting of the updated interface of the cast and the surface of the mold without its interface.

We adapt the cast mesh based on the surface deformation relative to the initial mold mesh using RBF interpolation-based mesh

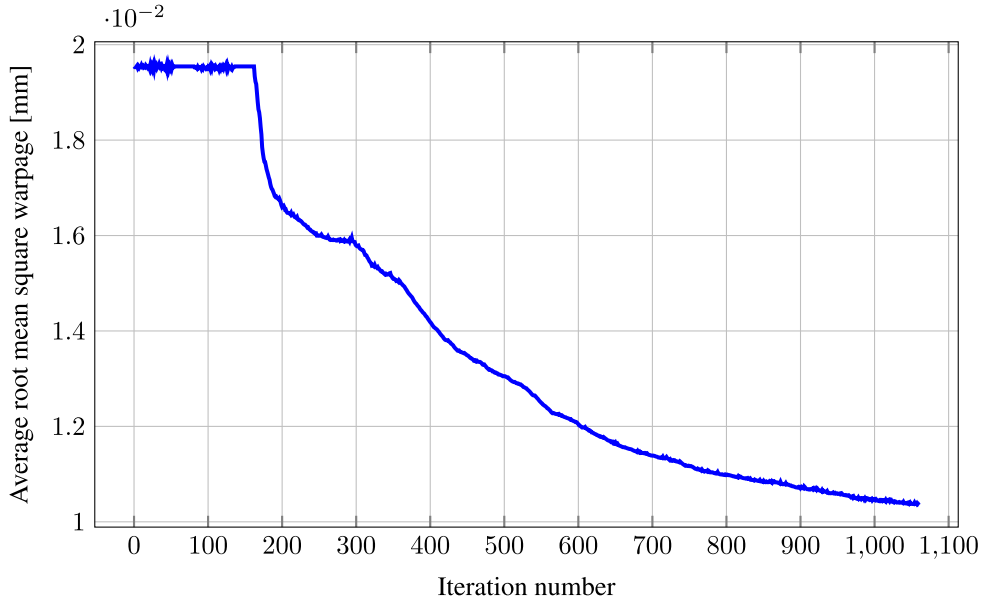

FIGURE 2 | Objective function value over iterations.

morphing. For this purpose, we utilize the Python library PyGem [39]. By providing the undeformed and deformed states of our RBF control points, we can apply the corresponding deformation to the mesh nodes. The RBF control points consist of two groups of nodes: first, the outer surface mesh nodes of the original mold, and second, the updated surface mesh nodes of the cast mesh from the next iteration. Combining these groups as the initial and deformed states allows us to initiate the mesh morphing process. This morphing achieves two key objectives for the mold mesh: it repositions the interface mesh nodes (which lack a direct counterpart on the cast mesh) and adjusts the inner mesh nodes to maintain high mesh quality. This method automates the adaptation process, enabling multiple iterations of the reverse geometry method to be performed efficiently.

3 | Results and Discussion

In this section, we compare the performance of the shape optimization and reverse geometry method. For evaluating the performance, we use the average root mean square difference between the surface mesh nodes of the compensated geometry compared to the ideal geometry, which is the same as the objective function defined in Equation (4).

First, we show the results of the shape optimization approach. We ran this algorithm for approximately 1000 iterations. We did not use a stopping criterion in this study, as we ran the algorithm for as long as reasonably possible. The decrease of the warpage over the iterations is shown in Figure 2. The average warpage at the start is $1.95 \cdot 10^{-2}$ mm. In the L-shaped geometry, many areas of the part have low warpage, which reduces the average, and only some areas have higher warpage (see Figure 4). For the first 180 iterations, the warpage does not decrease, which is the part in the COBYQA algorithm where all optimization parameters are modified by a small value to approximate the derivatives at the starting point. After that, the warpage drops significantly and continues decreasing until the 1000th iteration, reaching around $1.1 \cdot 10^{-2}$ mm, about half of the initial warpage.

Now we show the results from the reverse geometry method. We ran the reverse geometry method for 30 iterations. The convergence is shown in Figure 3; here, a logarithmic scale is used for the y-axis. The warpage drops significantly in the first iteration to around $1 \cdot 10^{-3}$ mm. It decreases more for the subsequent 20 iterations, and after that, the value experiences some numerical oscillations. Overall, the warpage was reduced by a factor of 200. The resulting shapes of the geometry are shown in Figure 4. In this figure, you can see the outlines of 2D slices at the middle of the L-shape. The ideal geometry is shown in black, which coincides in the figure with the resulting geometry after ten iterations of the reverse geometry method (yellow). The initial warpage and the compensated geometry are shown in purple and red, respectively. The zoomed-in section of the corner shows that the resulting geometry matches the ideal geometry well and that the compensated geometry changed the shape in the opposite direction of the warped geometry. This shows that the reverse geometry method, which works for injection molding warpage reduction, can also be applied to aluminum casting.

In comparison, both methods can reduce the total warpage. However, the computational cost for the shape optimization method is significantly higher, and the warpage reduction is less compared to the reverse geometry method. This matches the findings from [20], where the reverse geometry method needed significantly fewer iterations for better warpage reduction.

4 | Conclusion and Outlook

Our results show that simulation-based warpage compensation works for aluminum casting. The reverse geometry method reduced the warpage by two orders of magnitude with around 20 iterations. The shape optimization-based approach is much more expensive in terms of computational cost, but it is more

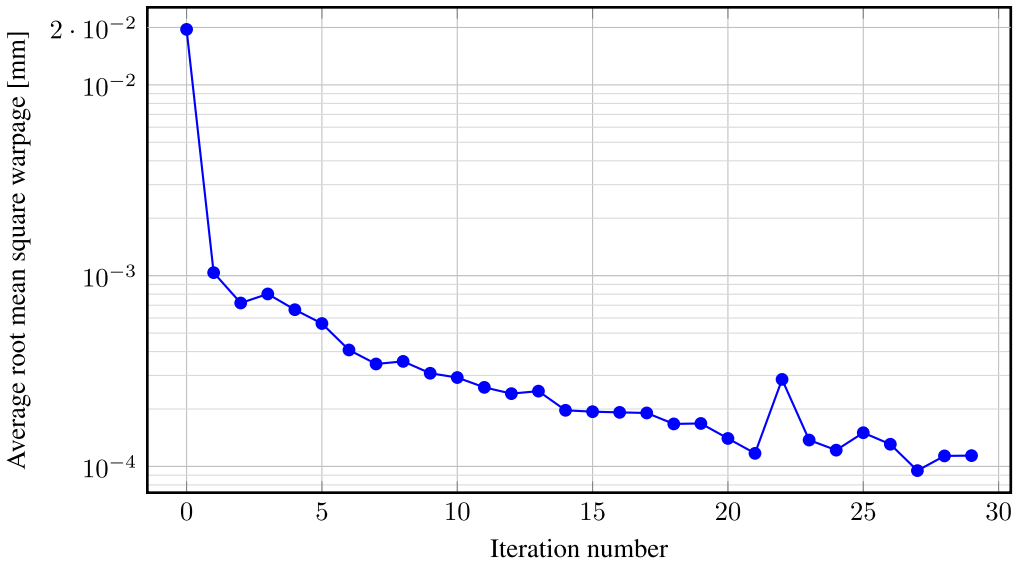

FIGURE 3 | Objective function value over iterations.

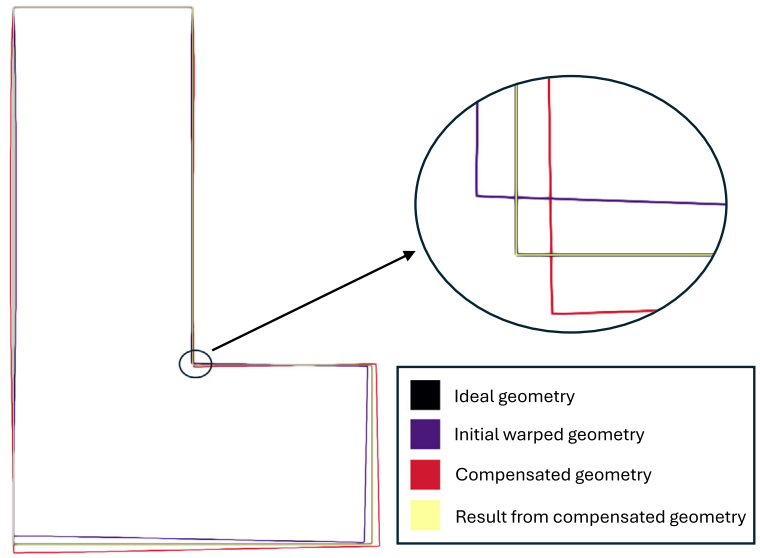

FIGURE 4 | Different 2D-slices of the L-shape geometry resulting from the reverse geometry method. The initial warpage is in purple, and the compensated geometry after ten iterations is in red. Note that the ideal geometry (black) and the result from the compensation (yellow) lie on top of each other.

general and allows additional goals to be incorporated into the optimization. In cases where only a geometric warpage reduction is needed, we strongly recommend the reverse geometry method. Still, the shape optimization method is useful when additional constraints or optimization goals are required.

Future research will apply the methods to a more complex simulation model. The current simulation model still has some simplifications. Additionally, we want to use the warpage compensation algorithms for more complex and realistic shapes compared to real-world application components. Both methods, especially the reverse geometry method, should perform similarly, regardless of the part's complexity. The shape optimization method will also be extended to account for additional optimization goals, like minimizing hot cracking tendencies, by incorporating it into the objective function of the shape optimization framework.

Acknowledgments

The presented investigations were carried out at RWTH Aachen University within the framework of the Collaborative Research "Centre SFB1120-236616214 Bauteilpräzision durch Beherrschung von Schmelze und Erstarrung in Produktionsprozessen" and funded by the Deutsche Forschungsgemeinschaft e.V. (DFG, German Research Foundation). The sponsorship and support are gratefully acknowledged. Computations were performed with computing resources granted by RWTH Aachen University under project rwth1259 and p0020502.

Open access funding enabled and organized by Projekt DEAL.

Data Availability Statement

The data and materials for this publication are available on request at the following link http://hdl.handle.net/21.11102/d29b8c45-e712-4583-b7fa-e5e7b7f2c005.

References

1. J. Campbell, *Complete Casting Handbook: Metal Casting Processes, Metallurgy, Techniques and Design* (Butterworth-Heinemann, 2015).

2. N. Wolff, T. Hohlweck, U. Vroomen, A. Bührig-Polaczek, and C. Hopmann, "Development of an Experimental Setup to Investigate Influences on Component Distortion in Gravity Die Casting and a First Variation of Temperature Control Strategy," *Metals* 11, no. 12 (2021): 2028, https://doi.org/10.3390/met11122028.

3. A. Hidayat, D. Rahmalina, and R. A. Rahman, "Impact of Top Mold Slope on Defect Formation in Gravity Casting of Aluminum Alloy," *Annales de Chimie Science des Matériaux* 48, (2024).

4. S. F. Hussainy, M. V. Mohiuddin, P. Laxminarayana, A. Krishnaiah, and S. Sundarrajan, "A Practical Approach to Eliminate Defects in Gravity Die Cast Al-Alloy Casting Using Simulation Software," *International Journal of Research in Engineering and Technology* 4, no. 1 (2015): 114–123.

5. J. Zhao, G. Cheng, S. Ruan, and Z. Li, "Multi-Objective Optimization Design of Injection Molding Process Parameters Based on the Improved Efficient Global Optimization Algorithm and Non-Dominated Sorting-Based Genetic Algorithm," *International Journal of Advanced Manufacturing Technology* 78 (2015): 1813–1826.

6. B. S. Heidari, E. Oliaei, H. Shayesteh et al., "Simulation Simulation of Mechanical Behavior and Optimization of Simulated Injection Molding Process for PLA Based Antibacterial Composite and Nanocomposite Bone Screws Using Central Composite Design," *Journal of the Mechanical Behavior of Biomedical Materials* 65 (2017): 160–176.

7. X. Wang, J. Gu, C. Shen, and X. Wang, "Warpage Optimization With Dynamic Injection Molding Technology and Sequential Optimization Method," *International Journal of Advanced Manufacturing Technology* 78 (2015): 177–187.

8. Y. Xu, Q. Zhang, W. Zhang, and P. Zhang, "Optimization of Injection Molding Process Parameters to Improve the Mechanical Performance of Polymer Product Against Impact," *International Journal of Advanced Manufacturing Technology* 76 (2015): 2199–2208.

9. N.-Y. Zhao, J.-Y. Lian, P.-F. Wang, and Z.-B. Xu, "Recent Progress in Minimizing the Warpage and Shrinkage Deformations by the Optimization of Process Parameters in Plastic Injection Molding: A Review," *International Journal of Advanced Manufacturing Technology* 120, no. 1-2 (2022): 85–101.

10. S. Kitayama, Y. Yamazaki, M. Takano, and S. Aiba, "Numerical and Experimental Investigation of Process Parameters Optimization in Plastic Injection Molding Using Multi-Criteria Decision Making," *Simulation Modelling Practice and Theory* 85 (2018): 95–105.

11. C. Hopmann and P. Nikoleizig, "Inverse Thermal Mold Design for Injection Molds: Adressing the Local Cooling Demand as Quality Function for an Inverse Heat Transfer Problem," *International Journal of Material Forming* 11 (2018): 113–124.

12. T. Hohlweck, D. Fritsche, and C. Hopmann, "Validation of an Extended Objective Function for the Thermal Optimisation of Injection Moulds," *International Journal of Heat and Mass Transfer* 198 (2022): 123365.

13. R. Azad and H. Shahrajabian, "Experimental Study of Warpage and Shrinkage in Injection Molding of HDPE/rPET/Wood Composites With Multiobjective Optimization," *Materials and Manufacturing Processes* 34, no. 3 (2019): 274–282.

14. B. Lee and B. Kim, "Variation of Part Wall Thicknesses to Reduce Warpage of Injection-Molded Part: Robust Design Against Process Variability," *Polymer–Plastics Technology and Engineering* 36, no. 5 (1997): 791–807.

15. S. Thiel, "Schneller zum perfekten Spritzgießwerkzeug," *Plastverarbeiter* 9 (2020).

16. C. Huang, C.-J. Yeh, G.-G. Lin, and W.-R. Jong, "Optimizing the Warpage of Injection Molding Parts Using 3D Volume Shrinkage Compensation Method," *SPE Technical Papers, Proceedings of the ANTEC Anaheim* (2017): 1575–1580.

17. F. Zwicke and S. Elgeti, "Inverse Design Based on Nonlinear Thermoelastic Material Models Applied to Injection Molding," *Finite Elements in Analysis and Design* 165 (2019): 65–76.

18. F. Zwicke, T. Hohlweck, C. Hopmann, and S. Elgeti, "Inverse Design Based on Nonlinear Thermoelastic Material Models," *Proceedings in Applied Mathematics and Mechanics* 20, no. 1 (2021): e202000130.

19. T. Kastelic, B. Starman, G. Cafuta, M. Halilovic, and N. Mole, "Correction of Mould Cavity Geometry for Warpage Compensation," *International Journal of Advanced Manufacturing Technology* 123, no. 5-6 (2022): 1957–1971.

20. S. Tillmann, S. Basermann, and S. Elgeti, "Comparison of Numerical Methods for Geometric Warpage Compensation,"International Journal for Numerical Methods in Fluids 97, no. 9 (2025): 1280–1288.

21. S. Tillmann, S. Schwan, D. C. Fritsche, C. E. Kahve, S. Elgeti, and C. Hopmann, "Using the Reverse Geometry Method for Warpage Compensation on Changing Meshes With Interpolation Methods," *Proceedings in Applied Mathematics and Mechanics* 24, no. 4 (2024): e202400010.

22. T. W. Sederberg and S. R. Parry, "Free-Form Deformation of Solid Geometric Models," in *Proceedings of the 13th Annual Conference on Computer Graphics and Interactive Techniques* (ACM SIGGRAPH, 1986), 151–160.

23. B. Shahriari, K. Swersky, Z. Wang, R. P. Adams, and N. De Freitas, "Taking the Human Out of the Loop: A Review of Bayesian Optimization," *Proceedings of the IEEE* 104, no. 1 (2015): 148–175.

24. S. Tillmann, M. Behr, and S. Elgeti, "Using Bayesian Optimization for Warpage Compensation in Injection Molding," *Materialwissenschaft und Werkstofftechnik* 55, no. 1 (2024): 13–20, https://doi.org/10.1002/mawe.202300157.

25. M. Alexa, "Recent Advances in Mesh Morphing," *Computer Graphics Forum* 21, no. 2 (2002): 173–198.

26. M. L. Staten, S. J. Owen, S. M. Shontz, A. G. Salinger, and T. S. Coffey, "A Comparison of Mesh Morphing Methods for 3D Shape Optimization," in *Proceedings of the 20th International Meshing Roundtable* (Sandia National Laboratories, 2012), 293–311.

27. A. De Boer, M. S. Van der Schoot, and H. Bijl, "Mesh Deformation Based on Radial Basis Function Interpolation," *Computers & Structures* 85, no. 11-14 (2007): 784–795.

28. M. E. Biancolini, "Mesh Morphing and Smoothing by Means of Radial Basis Functions (RBF): A Practical Example Using Fluent and RBF Morph," in *Handbook of Research on Computational Science and Engineering: Theory and Practice* (IGI Global, 2012), 347–380.

29. M. J. Powell, "Radial Basis Functions for Multivariable Interpolation: A Review," *Algorithms for Approximation* 6 (1987): 143–167.

30. B. Baxter, "The Interpolation Theory of Radial Basis Functions," *arXiv preprint arXiv:1006.2443* (2010).

31. N. Demo, M. Tezzele, A. Mola, and G. Rozza, "Hull Shape Design Optimization With Parameter Space and Model Reductions, and Self-Learning Mesh Morphing," *Journal of Marine Science and Engineering* 9, no. 2 (2021): 185.

32. C. B. Allen and T. C. Rendall, "CFD-Based Optimization of Hovering Rotors Using Radial Basis Functions for Shape Parameterization and Mesh Deformation," *Optimization and Engineering* 14 (2013): 97–118.

33. C. Groth, A. Chiappa, and M. Biancolini, "Shape Optimization Using Structural Adjoint and RBF Mesh Morphing," *Procedia Structural Integrity* 8 (2018): 379–389.

34. R. Cenni, C. Groth, and M. Biancolini, "Structural Optimisation Using Advanced Radial Basis Functions Mesh Morphing," in *Proceedings of the AIAS 44th National Congress*, vol. 503 (AIAS, 2015).

35. Abaqus User Manual, Simulia. "Abaqus 6.11," (2016): v6.

36. T. M. Ragonneau, "Model-Based Derivative-Free Optimization Methods and Software" (PhD thesis, Department of Applied Mathematics, The Hong Kong Polytechnic University, 2022).

37. T. M. Ragonneau and Z. Zhang, "COBYQA Version 1.1.2," (2024).

38. C. B. Sullivan and A. Kaszynski, "PyVista: 3D Plotting and Mesh Analysis Through a Streamlined Interface for the Visualization Toolkit (VTK)," *Journal of Open Source Software* 4, no. 37 (May 2019): 1450, https://doi.org/10.21105/joss.01450.

39. M. Tezzele, N. Demo, A. Mola, and G. Rozza, "PyGeM: Python Geometrical Morphing," *Software Impacts* 7,(2020): 100047, https://doi.org/10.1016/j.simpa.2020.100047.